Artefacts, Noise, Filtering and Compensation Techniques

Geoff JM Parker, PhD
Imaging Science and Biomedical Engineering, University of Manchester, Manchester, UK.

1. Introduction

Image and time series data are frequently used for quantitative purposes in many MRI studies. MRI has a major advantage over alternative imaging modalities due to the wide range of contrast mechanisms available and the equally wide range of sensitivities to the cellular environment and physiological processes (for example tissue water diffusion and tissue perfusion), thus extending the possibilities for quantitative imaging beyond the obvious candidates of volumetric measurement of organs and lesions. However, all imaging studies are hindered to some degree by image artefacts and signal noise, which degrade image quality. An image artefact may be defined as unwanted signal in an image, caused by confounding processes during data acquisition (for example patient motion). Signal noise is the random fluctuation of the measured image intensity around its true value and is ubiquitous to all measurement processes. These sources of degradation have two principal effects in quantitative studies: First, they obscure features in images that may be of interest. For example, accurate delineation of an organ for volume measurement may be impossible due to the presence of motion-induced artefact. Second, they can lead to measurements that are inaccurate (far from the true value), imprecise (demonstrating large fluctuations from measurement to measurement), or both.

This document summarises a small selection of the key sources of MR image artefact and noise and then introduces some of the key basic concepts related to image enhancement and restoration. One of the main reasons for enhancing image quality is to allow subsequent image feature extraction for quantification; an example of spatial feature extraction and an example of time series feature extraction are therefore presented. Whilst there is neither time nor space to cover all relevant analysis methods, those presented give a flavour of the role that such methods have in quantitative imaging studies, and include 'pure' image analysis methods in addition to methods more specific to quantitative MRI analysis. These concepts are put into context with the aid of examples of advanced quantitative applications that require these at an early stage or as an integral part of the analysis.

2. Sources of Artefact and Noise

Artefacts present in MR images are often dependent on the details of the image acquisition sequence. A comprehensive description of all artefacts and their sources is far beyond the scope of this document. However, some of the commonest artefacts in clinical imaging include those due to subject motion, field inhomogeneities, and inadequate sampling of k space:

2.1. Motion

Phase encoded images rely on consistent positioning of the object being imaged between the acquisition of each line, or segment, of k space. Any motion between each acquisition will lead to information being incorrectly encoded in k space. The resulting image, formed using a Fourier transform of the k space data, will then demonstrate spatially offset signal and/or blurring artefacts along the phase encoding direction of the image (parts of which may also be misaligned in the frequency or slice encoding directions, dependant on the pattern and magnitude of motion). Note that relatively small amounts of motion can lead to relatively large artefacts in the phase encode direction.

2.2. Field Inhomogeneities

One of the primary causes of signal intensity non-uniformity is inhomogeneity in the RF fields associated with imaging coils in both transmission and receive mode. Transmit RF non-uniformity leads to variable flip angles across images (which can affect contrast weighting in addition to gross signal intensity). The coil sensitivity profile will dictate the distribution of signal intensity by a spatially-varying scaling factor. In clinical radiological imaging spatial signal variation seldom leads to severe degradation of diagnostic utility. However, the same non-uniformity can have a severe impact on quantitative analysis. For example, relaxation time measurements relying on accurate estimates of flip angle, or volume estimates relying on accurate classification of tissues according to their signal intensities are severely affected by the presence of RF field inhomogeneities.

The effect of static field (B_0) inhomogeneities is highly dependent on the pulse sequence being used. 'Conventional' spin echo or gradient echo acquisitions are to a large extent unaffected by the levels of B_0 inhomogeneity present in modern clinical scanners. However, rapid acquisition techniques, such as echo planar imaging (EPI) are sensitive to the small non-uniformities associated with magnetic susceptibility changes at tissue boundaries. This may be manifest as geometric distortion, which will confound volume measurements, and signal

drop out, which will reduce the signal to noise ratio (SNR), and which can have an impact on, for example, the statistical power of an fMRI analysis.

2.3. Inadequate Sampling of K Space

The requirement for rapid data acquisition in many imaging studies necessitates the rapid filling of k space. A number of strategies exist for achieving this, including the reduction of the acquisition matrix size and the use of methods to fill part of k space using (possibly) redundant image information, such as half-Fourier and 'keyhole' techniques ((1) provides a good overview of these methods, and sequence design in general, including sources of artefact). Whilst such methods are very useful, they lead to a number of commonly observed artefacts. For example, a small imaging matrix with large in-plane voxel dimensions will exhibit a noticeable point spread function – a phenomenon known as Gibbs ringing.

2.4. Noise

Two types of noise exist in MR images – 'system' noise and physiological noise. The former is independent of the object being imaged (it could equally be a phantom or a patient) and is caused primarily by thermal noise in the subject and in the electrical circuitry of the scanner, in particular the RF coil. A number of physical imaging parameters affect the level of system noise in an image: the voxel size, the number of data averages, the number of phase encoding lines, the size of the imaging coil, the pulse profile, the field strength, and the interaction between tissue relaxation times and sequence parameters such as TE and TR. Physiological noise is effectively artefactual signal caused by processes such as blood and CSF pulsation and breathing-related motion that leads to random (or apparently random) spatial and frequency variation in the image.

3. Image Enhancement

Reducing the impact of artefacts and image noise may allow increased measurement accuracy and/or precision. Filtering methods for noise reduction and methods for reducing the effects of field non-uniformity are presented as examples of useful post-processing image enhancement methods.

3.1. Noise Reduction

It is essential to ensure that the data acquisition is optimized for the task in hand. The noise levels in the acquisition are a key element in this optimization, and should not be overlooked. However, often there are equally compelling data acquisition requirements, such as limited scan time or an upper limit on image spatial resolution, that compete with the need for high SNR. Post-processing techniques may be of use in reducing the detrimental effects of noise in these situations.

Reductions in image noise may be achieved by the use of spatial filters applied to the image. Typically this is achieved by defining a mask that allows voxels within a specified image neighbourhood (or equivalently neighbouring points in time in a time series) to modulate the signal intensity within the voxel at the mask's centre, a process that is applied to each image voxel in turn. The mask contains weighting coefficients that define the influence that neighbouring voxel intensities will have on the current working voxel, according to

$$I' = \sum_{n=1}^{N} w_n I_n \quad , \qquad \sum_{n=1}^{N} w_n = 1 \tag{1}$$

where I' is the modified signal intensity at the current working voxel, w_n is the mask weighting coefficient at neighbourhood voxel n, I_n is the voxel signal intensity at the mask location n. The simplest such filter is the mean filter, which has equal values for all w_n (Fig. 1).

A range of filters may be constructed using this approach, which can be grouped, in terms of the spatial frequency information that they preserve, into lowpass, highpass, and bandpass filters. Lowpass filters generally reduce image noise by restricting the high spatial frequency information in the image. The simplest of these is the mean filter, which reduces the high spatial frequency image noise by a simple averaging of local signal intensities (Fig. 2). However, alternative weighting schemes exist, an important example of which is Gaussian weighting (giving what is commonly known as "Gaussian smoothing") (Fig. 2).

w_1	w_2	w_3
w_4	w_5	w_6
w_7	w_8	w_9

a

1/9	1/9	1/9
1/9	1/9	1/9
1/9	1/9	1/9

b

1/25	1/25	1/25	1/25	1/25
1/25	1/25	1/25	1/25	1/25
1/25	1/25	1/25	1/25	1/25
1/25	1/25	1/25	1/25	1/25
1/25	1/25	1/25	1/25	1/25

c

Figure 1. (a) General form of a 3x3 linear filter mask. (b) 3x3 mean filter, including weights. (c) 5x5 mean filter, including weights.

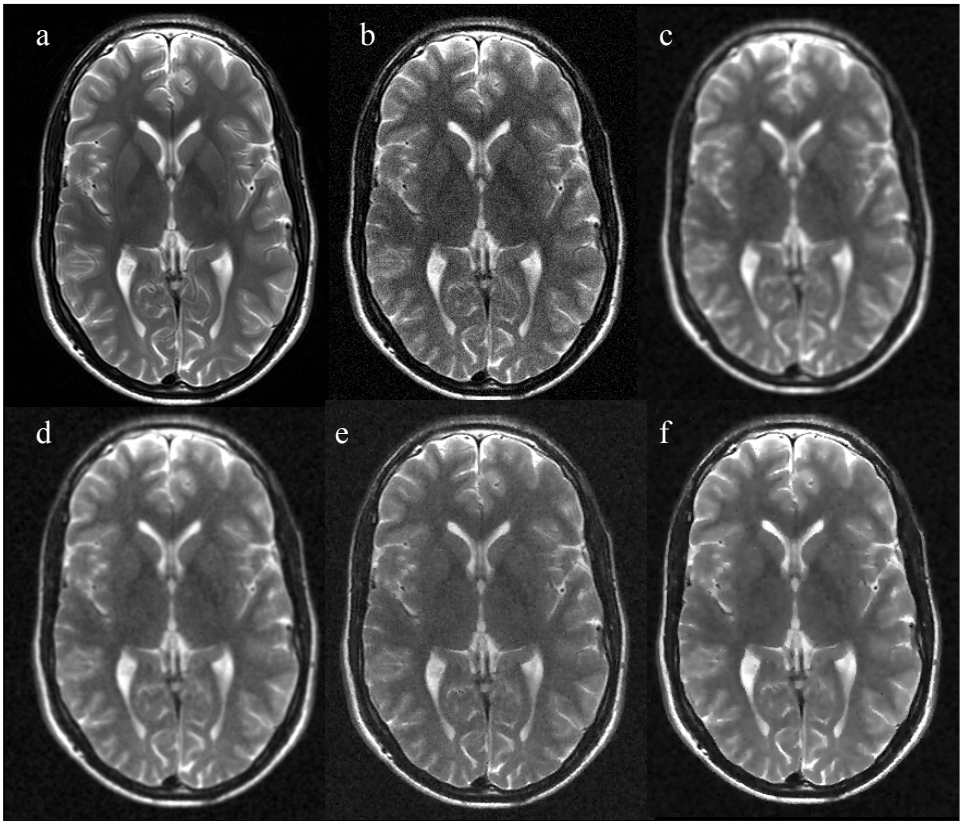

Figure 2. The effects of filtering in 2D. (a) original image; (b) image corrupted with Gaussian noise; (c) effect of 3x3 mean filter; (d) effect of Gaussian filter with an effective standard deviation of 2 pixels; (e) anisotropic diffusive filtering, 5 iterations; (f) anisotropic filtering, 10 iterations.

Both the mean and Gaussian filters are effective at reducing image noise, but at the expense of introducing significant blurring of the interfaces between tissues (Fig. 2). More sophisticated filtering schemes have been introduced that aim to maintain noise-reduction, whilst affecting the interfaces between tissues less. One such method is the "anisotropic diffusion" filter introduced by Perona and Malik (2). This filter works by identifying edge structure in the image (see section 4.1), and performing smoothing only in areas away from the edges. If a Gaussian filter can be thought of as applying an isotropic diffusive effect on image signal intensity (i.e. blurring), the

anisotropic diffusion filter can be thought of as restricting the diffusion process across image edges, thus preserving structural information, with the change in image signal intensity due to the smoothing defined by:

$$\frac{\partial I(x,y,t)}{\partial t} = div\left[g\left(\left\|\underline{\nabla} I\right\|\right)\underline{\nabla} I \right] \\ g\left(\left\|\underline{\nabla} I\right\|\right) = \exp\left(-\left(\left\|\underline{\nabla} I\right\|/K\right)^2\right) \quad (2)$$

where K is a control constant and $\underline{\nabla} I$ is the spatial gradient in signal intensity (see section 4.1), and t is an artificial time parameter, analogous to the number of iterations of the filter that are applied.

Image filtering is often performed directly on the image, but is often equally applicable in spatial frequency space (i.e. k space). A low pass filter in image space is analogous to discarding high frequency components in k space.

Noise reduction has application in quantitative image and data analysis to reduce both random and systematic errors. Whilst it is straightforward to see how random errors may be reduced by noise reduction, the reduction in systematic errors is less obvious. One example has been the use of anisotropic smoothing in diffusion tensor imaging, where systematic errors are introduced into measurements of diffusion anisotropy by noise (3, 4). Figure 3 demonstrates the reduction of bias in fractional anisotropy (FA) via the application of noise reduction (4).

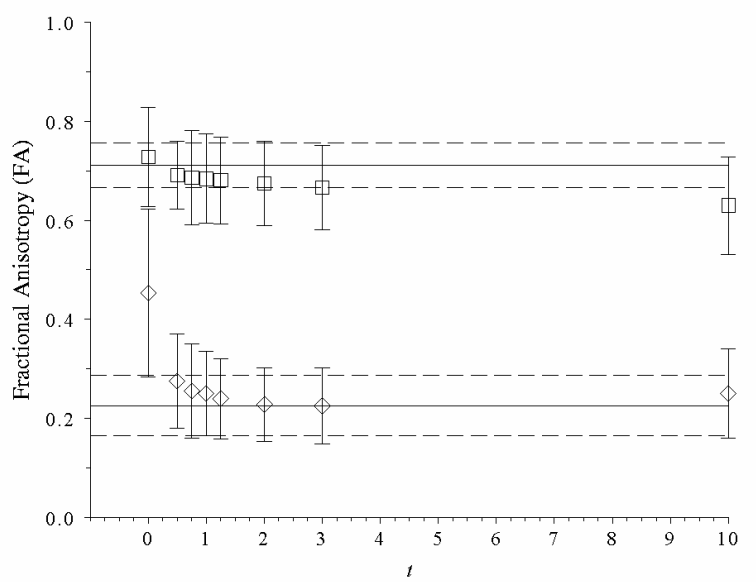

Figure 3. Change in FA in white matter (squares) and grey matter (diamonds) with progressive amounts of anisotropic smoothing. Solid lines represent uncorrupted values within regions of interest; dashed lines represent ±1 standard deviation.

3.2. Non-uniformity Correction

RF fields Both the transmission RF and the receive RF fields contribute to the observed non-uniformity. Correction for receive field non-uniformity is becoming standard on modern scanners (a spin-off parallel imaging processing). This generally works by defining the receive sensitivity profile of a coil by acquiring one image with the coil in question being used for reception and a second image with the scanner body resonator (which, due to its size, can be assumed, to a good approximation, to be uniform) being used for reception. A simple division of the signal intensities resulting from the two images yields the coil receive sensitivity profile, which can then be used to correct all images acquired with this coil during the patient visit.

Transmission RF non-uniformity may be compensated for using B_1 mapping techniques (5). This requires the use of multiple flip angle data acquisitions and a knowledge of the expected relationship between signal intensity and pulse sequence flip angle (for a detailed review see (6)).

Purely image-based, retrospective methods have been proposed to remove RF-induced non-uniformity (for a comparison of some available methods see (7)). These generally work on the principle that RF field-induced inhomogeneity (whether in transmit or receive) is a low spatial frequency effect, which can therefore be distinguished from signal intensity variations due to tissue contrast, which, generally, occur at higher spatial

frequencies. Two main classes of methods have been proposed for exploiting this. The first is to utilize low pass filtering of the image to estimate the low spatial frequency variation of the RF field (see for example (8)). A second class attempts to estimate a bias field that reduces the variance in the histograms of signal intensities for different tissue types, under the assumption that given no non-uniformity the peaks corresponding to different tissues will have their minimum (correct) width (see for example (9)).

Most applications of non-uniformity correction to date have been in neuroimaging (see for example (7)). However the methods are generic, and have been proven also in body imaging (see for example (10)).

$\underline{B_0}$ The static magnetic field is far more uniform than the RF fields associated with imaging coils. However, low bandwidth acquisitions, such as echo planar imaging (EPI) are sensitive to the small non-uniformities associated with magnetic susceptibility changes at tissue boundaries. Susceptibility distortions can be reduced with the use of an explicitly measured B_0 field (11), or for spin echo EPI with the use of two separate data acquisitions with opposite readout gradient polarity, each of which has the distortions in the opposite sense (12, 13). The main drawback of such approaches is the requirement for additional data acquisition to enable the correction. Post-processing options include non-linear registration of the distorted EPI image to an undistorted reference image.

4. Feature Extraction

Automated data analysis techniques such as segmentation may require the definition of features within the image to form the basis of the outline of specific structures.

4.1. Edge detection

The concept of an image mask introduced in section 2.1 is applicable to the identification of image features, such as points, lines, or image edges (for an overview, see for example (14)). The key element in extracting this information is the definition of the local gradient in image intensity within an image, based on the assumption that the edge in question is the boundary between two regions with relatively distinct signal intensities. The gradient can be defined (for simplicity in 2 dimensions):

$$\underline{\nabla} I(x,y) = \begin{bmatrix} G_x(x,y) \\ G_y(x,y) \end{bmatrix} = \begin{bmatrix} \dfrac{\partial I(x,y)}{\partial x} \\ \dfrac{\partial I(x,y)}{\partial y} \end{bmatrix}. \tag{3}$$

The most straightforward calculation of the gradient within the discretely sampled MR image is as the difference between neighbouring voxel intensities. However, more robust estimations of the gradient can be achieved using the Sobel filter (Fig. 4), applied in the same way as the masks in Fig. 1. In practice, the differential operation required to generate the image gradient is sensitive to image noise, and a small amount of noise reduction (usually Gaussian

a

-1	0	-1
-2	0	-2
-1	0	-1

-1	-2	-1
0	0	0
-1	-2	-1

b

Figure 4. Sobel filter masks, including weights. (a) G_x, (b) G_y.

smoothing) is usually applied before extracting the gradient information (Fig. 5b). To identify an edge in an image we are not interested in the sign of the gradient, so the gradient magnitude is usually employed (Fig. 5c). However, this does not localize the edges precisely, as changes between tissue types are often spread over a few voxels. This is overcome by using non-maximal suppression of local gradients (Fig. 5d). Further refinement of the technique via a process known as hysteresis thresholding allows the use of neighbourhood information to connect segments of edge, whilst avoiding noise-induced information (the net result is known as the Canny edge detector (15) (Fig. 5e)).

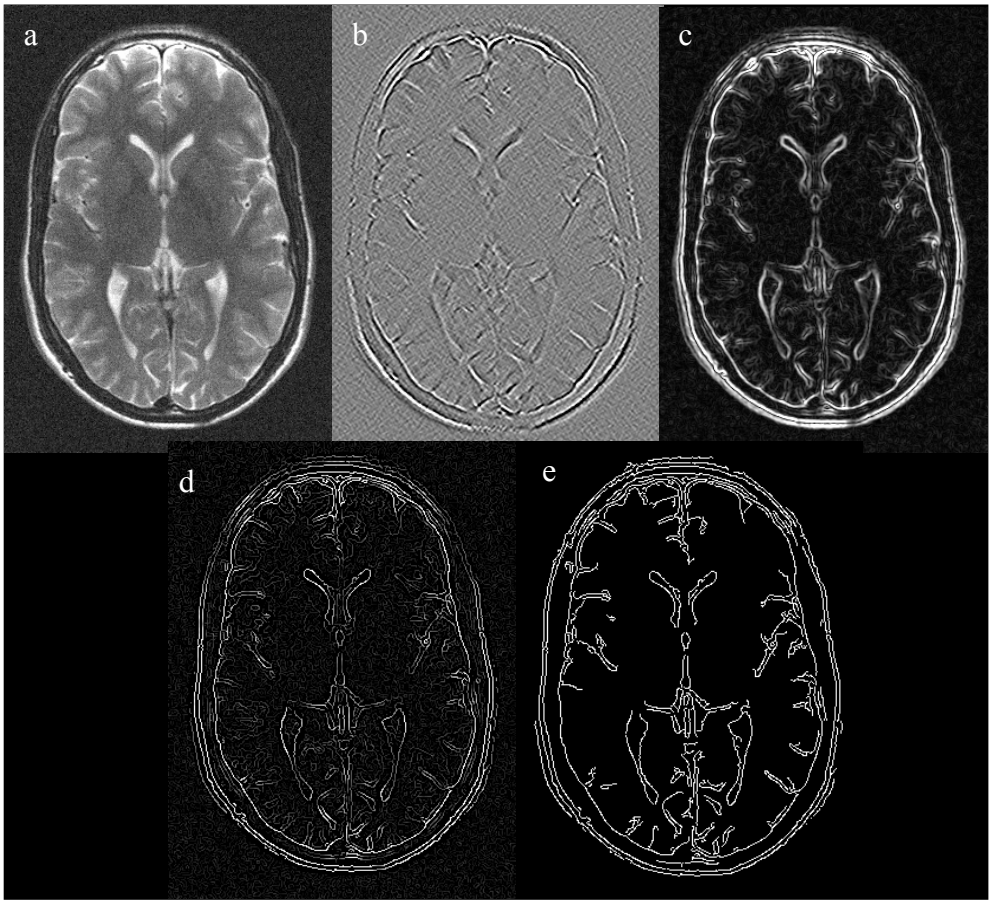

Figure 5. Steps in edge detection. (a) original, noisy image; (b) gradient image; (c) gradient magnitude; (d) gradient image with non-maximal gradient suppression; (e) final result of Canny edge detection after hysteresis thresholding.

4.2. Principal components analysis (PCA)

A useful technique for extracting features from images or time series data without imposing any prior knowledge on the data content is principal components analysis (PCA). PCA takes multidimensional data (for example a time series of images) and reduces it to axes of uncorrelated data. The first PCA axis will describe the mode of variation with most variance in the image data. The second axis will have the next most variance, etc. The fact that each principal component is defined to be orthogonal means that each contains entirely independent information. In time series studies it is possible to generate images of the magnitude of the variation associated with each component (eigenimages). Features that occur strongly in different eigenimages will have distinctly different signal intensity time courses. PCA and the related area of independent components analysis (ICA) have application in fMRI and dynamic contrast enhanced MRI (DCE-MRI) analysis. Figure 6 shows an example of PCA analysis applied to a T_1-weighted DCE-MRI time series in the abdomen. The individual principal component eigenimages identify different tissues, each with a characteristic time course of signal change in response to intravenous contrast agent administration.

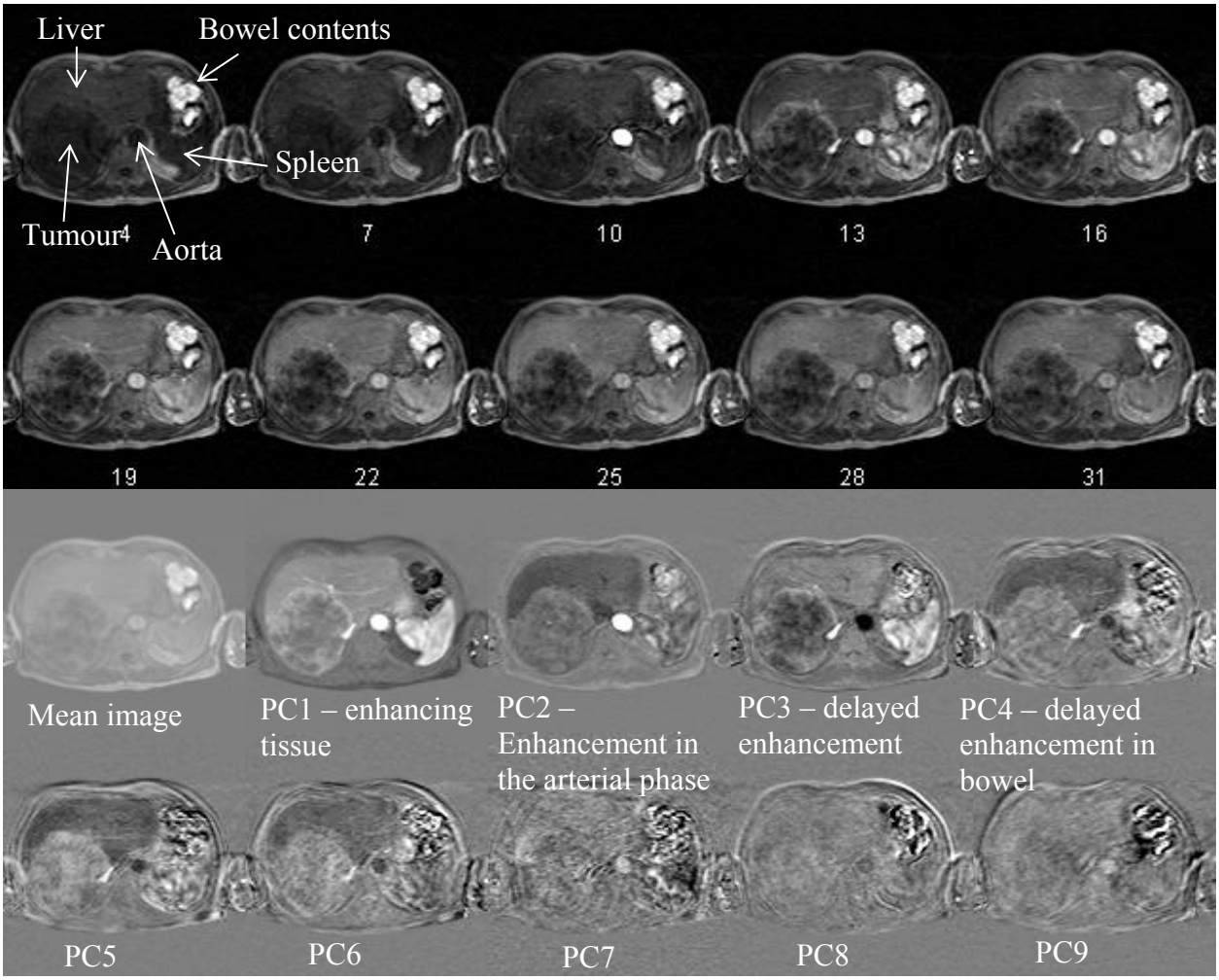

Figure 6. PCA analysis in a DCE-MRI time series in a liver tumour. Top: time series showing signal change due to arrival of contrast agent (number indicate image index). Bottom; Mean time series image plus first 9 principal component (PC) eigenimages. The approximate physical interpretation is given, where appropriate.

References

1. Bernstein MA, King KF, Zhou XJ. *Handbook of MRI pulse sequences* (Elsevier Academic Press, Burlington, MA, 2004).
2. Perona P, Malik J. Scale-space and edge detection using anisotropic diffusion. IEEE Transactions on Pattern Analysis and Machine Intelligence 1990;12:629-639.
3. Pierpaoli C, Basser PJ. Toward a quantitative assessment of diffusion anisotropy. Magn Reson Med 1996;36:893-906.
4. Parker GJM, Schnabel JA, Symms MR, Werring DJ, Barker GJ. Nonlinear image smoothing for reduction of systematic and random errors in diffusion tensor imaging. J Magn Reson Imag 2000;11:702-710.
5. Barker GJ, Simmons A, Arridge SR, Tofts PS. A simple method for investigating the effects of non-uniformity of radiofrequency transmission and radiofrequency reception in MRI. British Journal of Radiology 1998;71:59-67.
6. Tofts PS. in *Quantitative MRI of the brain - measuring changes caused by disease* (ed. Tofts, PS) 17-54 (John Wiley & Sons Ltd, Chichester, 2003).
7. Arnold JB, Liow J-S, Schaper KA, Stern JJ, Seld JG, Shattuck DW, Worth AJ, Cohen MS, Leahy RM, Mazziota JC, Rottenberg DA. Qualitative and quantitative evaluation of six algortims for correcting intensity nonuniformity effects. NeuroImage 2001;13:931-943.
8. Brinkmann BH, Manduca A, Robb RA. Optimized homomorphic unsharp masking for MR grayscale inhomogeneity correction. IEEE Trans Med Imaging 1998;17:161-171.

9. Ashburner J, Friston KJ. Voxel-based morphometry - the methods. Neuroimage 2000;11:805-821.
10. Vokurka EA, Thacker NA, Jackson A. A fast model independent method for automatic correction of intensity nonuniformity in MRI data. J Magn Reson Imag 1999;10:550-562.
11. Jezzard P, Balaban RS. Correction for geometric distortion in echoplanar images from B0 variations. Magn Reson Med 1995;34:65-73.
12. Bowtell R, McIntyre DJO, Commandre M-J, Glover PM, Mansfield P. Correction of geometric distortion in echo planar images. 2nd Meeting of the Society of Magnetic Resonance 1994;411.
13. Andersson JLR, Skare S, Ashburner J. How to correct susceptibility distortions in spin-echo echo-planar images: application to diffusion tensor imaging. NeuroImage 2003;20:870-888.
14. Gonzalez RC, Woods RE. *Digital image processing* (Addison-Wesley Publishing Company, Inc., Reading, 1993).
15. Canny J. A computational approach to edge detection. IEEE Transactions on Pattern Analysis and Machine Intelligence 1986;8:679-698.